| | |
|---|---|
| Title | Amorphous Silicon Schottky and MIS Solar Cells by rf Sputtering and rf Glow Discharge Decomposition |
| Author(s) | Moniwa, Masahiro; Yamamoto, Hidekazu; Hasegawa, Hideki |
| Citation | Memoirs of the Faculty of Engineering, Hokkaido University, 15(4), 487-498 |
| Issue Date | 1981-12 |
| Doc URL | http://hdl.handle.net/2115/37997 |
| Type | bulletin (article) |
| File Information | 15(4)_487-498.pdf |

# Amorphous Silicon Schottky and MIS Solar Cells by rf Sputtering and rf Glow Discharge Decomposition

**Masahiro MONIWA[*], Hidekazu YAMAMOTO[*] and Hideki HASEGAWA[*]**

(Received June 30, 1981)

## Abstract

For the production of low-cost terrestrial solar cells, formation of hydrogenated amorphous silicon films was investigated in detail and applied to the fabrication of Schottky and MIS solar cells.

Amorphous silicon (a-Si) films were formed by rf reactive sputtering of Si in $H_2+Ar$ and by rf glow discharge decomposition of $SiH_4$, using the same discharge chamber. It was found that a-Si films with high photoconductivity comparable to that of glow discharge films, can be obtained by rf sputtering under optimum conditions.

Au/a-Si Schottky and MIS solar cells were then fabricated. Anodization was used for thin insulator formation, using a glycol solution of $KNO_3$ as the electrolyte. Energy conversion efficiency of glow-discharge a-Si Schottky cells was found to be approximately ten times larger than that of optimized rf sputterd Schottky cells. An increase of open circuit voltage was achieved in anodized MIS cells and this was explained by an increase of semiconductor barrier height.

## 1. Introduction

Application of terrestrial solar cells are expected to increase sharply owing to world-wide shortage of energy, provided that their cost is reduced down to an acceptable one. In this respect, thin film solar cells using amorphous silicon (a-Si) are particularly promising. Attractive features of a-Si as the solar cell material can be summarized as follows:

(1) a-Si can be prepared at a relatively low temperature (200-350°C), thus avoiding power-consuming high-temperature processes that are typical in the single-crystal growth.

(2) Single-crystal semiconductor substrates are not required for a-Si film preparation. A variety of materials such as glass, ceramics, stainless steels etc. can be used.

(3) Thin films with large areas can be produced.

(4) The required thickness of a-Si solar cell operation is much smaller than those for single-crystal and poly-crystal Si solar cells because of the increased opti-

---

[*] 電気工学科，電気物性工学講座

[*] Materials Research Laboratory, Department of Electrical Engineering, Faculty of Engineering, Hokkaido University, Sapporo, 060 Japan.

cal absorption coefficient of a-Si in the wavelength region from 4000 to 7000Å⁽¹⁾. The required thickness for solar cell operation is typically 1 $\mu$m for a-Si cells, whereas a thickness more than 100$\mu$m is required for single-crystal or poly-crystal Si cells. GaAs solar cells requires a thickness of about 5 $\mu$m.

Owing to the above features, it is expected that the cost of a-Si solar cells can be reduced down to below a few % of that of present commercial single-crystal Si cells.

In addition to reduction of the material cost, the process cost for solar cell fabrication must also be reduced. As compared with the conventional p-n junction cell, the Schottky barrier solar cell can clearly be fabricated at a lower cost. And its open-circuit voltage is considerably smaller than that of p-n junction solar cell. Recent studies by many workers⁽²⁾ have shown that the open-circuit cell voltage of a Schottky barrier solar cell can be remarkably increased by introducing a thin insulating layer between the metal and semiconductor by the use of a suitable process. This type of solar cells are called MIS (Metal Insulator Semiconductor) solar cells.

In the present paper, the electrical and photoelectrical properties of the hydrogenated a-Si (a-Si: H) thin films prepared by rf reactive sputtering of Si and by rf glow discharge decomposition of silane ($SiH_4$) described. The film deposition parameters were optimized to maximize the ratio of the photoconductivity to the dark conductivity. Schottky and MIS solar cells were then fabricated using optimized a -Si: H films. The formation of insulating layer for MIS cells were done by anodic oxidation (anodization) with reference to recent promising results reported on GaAs, InP and Si single-crystal anodized MIS solar cells by our group.⁽³⁾,⁽⁴⁾ Since the photoelectrical properties of a-Si: H films show degradation at high temperatures above 500°C, owing to dissociation of hydrogen, a low-temperature process such as anodization seems to be particularly attractive for a-Si: H films. A somewhat promising result was obtained in this regard by the present study.

## 2. Preparation and Properties of a-Si: H Films

Amorphous silicon films can be prepared by various processes such as vacuum evaporation, rf sputtering, ion beam sputtering, chemical vapor deposition, glow or arc discharge decomposition of monosilane or silicon tetrafluoride, etc.. However, in order to obtain a practical useful solar cell operation, reduction of localized gap state density is essential, and this can be achieved by incorporation of hydrogen atoms as was demonstrated by the pioneering works of " Dundee group "⁽⁵⁾ and " RCA group "⁽¹⁾, using glow-discharge decomposition of monosilane.

In the present study, hydrogenated a-Si (a-Si: H) films were prepared both by rf reactive sputtering of Si and decomposition of monosilane, using the same commercial rf sputtering apparatus (ULVAC, model SBR-1104E). Electrode and gas arrangements for both types of film deposition are illustrated in Fig.1 (a) and (b), respectively.

In order to measure the electrical properties of a-Si: H films, the samples were prepared in the so-called gap cell configuration, shown in Fig.2. a-Si layers, about

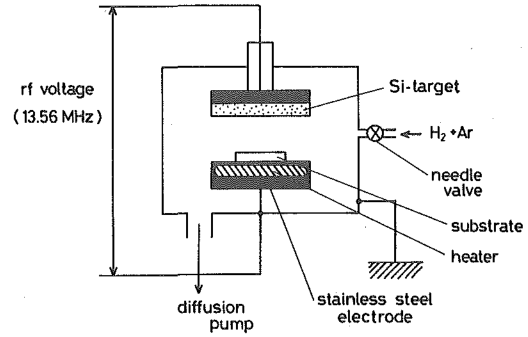

(a) rf sputtering of Si

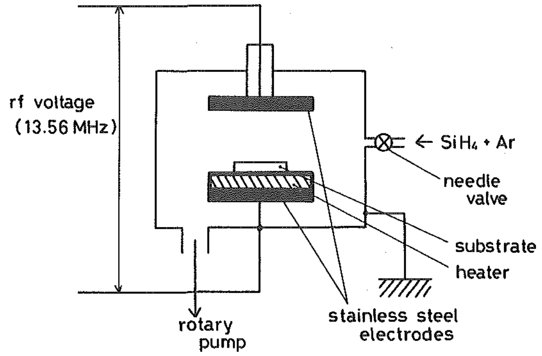

(b) rf glow discharge decomposition of silane

**Fig. 1** Electrode and gas arrangements of a-Si formation

8000Å thick, were deposited on glass substrates. The film thickness was determined by an interference microscope. Al–Al electrodes were evaporated onto a-Si films and provided contacts that resulted in linear current–voltage characteristics over a range of steady-state electric field strength from 50 to 300Vcm$^{-1}$, used in the present experiment. The current under dark and illuminated conditions were measured at room temperature with an electrometer (Keithley, model 610C). The room tempera-

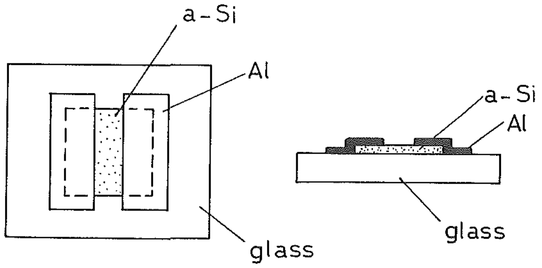

**Fig. 2** Sample shape for electrical characterization (gap cell configuration)

ture dark conductivity $\sigma_{\mathrm{dark}}$ and the ratio of photoconductivity to dark conductivity $\sigma_{\mathrm{photo}}/\sigma_{\mathrm{dark}}$ at room temperature of the samples were investigated, where the photoconductivity $\sigma_{\mathrm{photo}}$ is defined as the difference between illuminated conductivity and dark conductivity. Illumination was provided by a collimated tungsten lamp of 70000*lx*.

### 2. 1 a-Si : H Films by Reactive Sputtering

Reactive rf sputtering of Si was carried out in a mixture of Ar and $H_2$ gases, using a non-dope poly-crystal Si target. The total gas pressure was kept at $1\times10^{-2}$ Torr to maintain a stable glow discharge, and the frequency of plasma was 13.56MHz.

Figure 3 shows the measured dependence of the dark conductivity and the ratio of photoconductivity to dark conductivity at room temperature on the hydrogen partial pressure of mixed gas for a fixed rf power of plasma of 150 W(1.9W/cm$^2$) and a substrate temperature of about 120°C. The deposition rate was about 1.4Å/sec. As seen in Fig.3, a maximum and a minimum of the dark conductivity were observed at the hydrogen pressure fraction of 0% and 20%, respectively. As for the ratio of photoconductivity to the dark conductivity, the largest value was obtained at the hydrogen fraction of 20%, as seen in Fig.3, taking a value of about 3. This result seems to suggest that the most favorable hydrogen pressure fraction for deposition of photo-sensitive a-Si films is 20% in the present system.

Figure 4 shows the measured rf power dependence of the room temperature photoconductivity $\sigma_{\mathrm{photo}}$ for four different hydrogen pressure fractions of 10, 20, 30 and 50%. rf power was varied from 50W (0.64 W/cm$^2$) to 500W (6.4 W/cm$^2$), and the deposition rate of a-Si films changed approximately from 1 Å/sec to 8 Å/sec as the

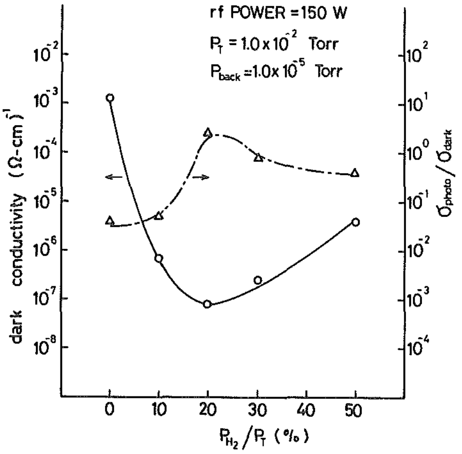

**Fig. 3** The measured dependence of dark conductivity and ratio of photoconductivity to dark conductivity on hydrogen pressure fraction

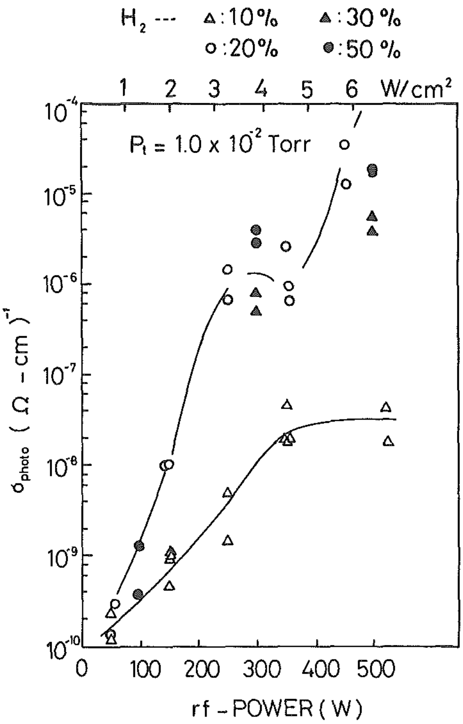

**Fig. 4** Plot of Photoconductivity vs. rf. power of sputtering

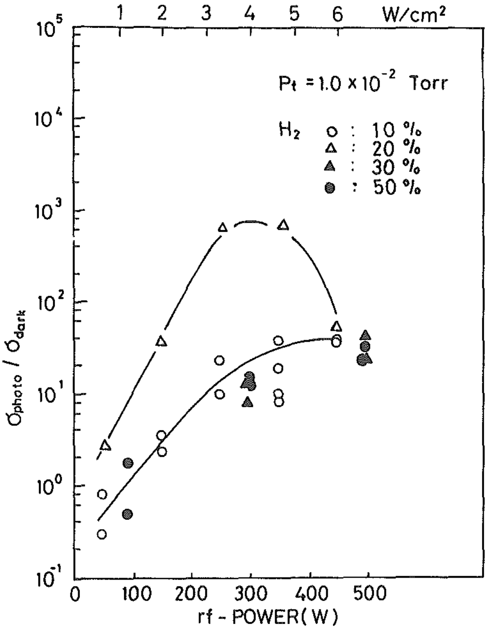

**Fig. 5** Plot of ratio of photoconductivity to dark conductivity vs. rf power of sputtering

power was increased within this range. As seen in Fig.4, the photoconductivity increases monotonically with the rf power in all cases, but for a fixed rf power, it is quickly saturated to a constant value, as the hydrogen pressure fraction is increased, resulting in the same curve for pressure fractions of 20, 30 and 50%.

The measured ratio, $\sigma_{\mathrm{photo}}/\sigma_{\mathrm{dark}}$, of photoconductivity to dark conductivity is plotted in Fig.5 vs. rf power for the same values of the hydrogen pressure fraction as in Fig.4. Here, the behavior of $\sigma_{\mathrm{photo}}/\sigma_{\mathrm{dark}}$ is clearly different between the case of hydrogen pressure fraction of 20% and the rest. In the latter cases of 10, 30 and 50%, the ratio increases monotonically but slowly with the increase of rf power, whereas a peak is clearly observed in the case of 20%, giving a peak values of a ratio as high as $0.8\times10^3$, at rf power of 300W (3.8 W/cm$^2$) and substrate temperature of 180°C. Thus, optimum conditions to achieve photosensitive films exist. It appears to be related to the optimum hydrogen incorporation with low plasma energy. Higher rf power increases the photoconductivity, but the dark conductivity also increases by enhanced hopping conduction due to increased gap-state density. The empirical optimum sputtering conditions obtained here differ, however, from those reported by other workers(6)(7), and this suggests that the optimum sputtering conditions in terms of the conventional parameters are perhaps different from one system to another, because of their inadequecy to specify plasma properties.

### 2. 2 a-Si : H Films by Glow-Discharge Decomposition and Comparison of Two Deposition Methods

Using the same sputtering apparatus, a-Si : H films were prepared by rf glow discharge decomposition of silane ($SiH_4$) diluted with argon ($SiH_4$:10%). Since extensive studies have already been made concerning this process by various workers, a standard choice was made for the deposition parameters. The flow rate of the $SiH_4$-Ar mixed gas was fixed at about 60 std. $cm^3$/min. The gas was continuously pumped away and the residual pressure of 2.5 Torr was maintained in the chamber. The glow discharge plasma was excited by rf power of 20 W (0.25 W/$cm^2$) with the frequency of 13.56 MHz between two stainless steel electrodes. The substrate temperature was 270°C and the spacing of the electrodes was 3.5cm. The resulting deposition rate of a-Si film was 1-2 Å/sec.

The measured $\sigma_{dark}$ and $\sigma_{photo}/\sigma_{dark}$ at room temperature are summarized and compared with the results of the rf sputtering method in Table 1. The reproducibility of electrical and photoelectrical properties of a-Si : H prepared by rf glow discharge technique were found to be much better than the rf reactive sputtering technique. However, the photoconductivity value achieved here by rf reactive sputtering is comparable to that by glow discharge decomposition, and is much higher than the value previously reported(8). Thus it is surmised that further work may lead to further improvements.

**Table 1** Comparison of dark- and photo-conductivity of a-Si films

| | $\sigma_{dark}$ | $\sigma_{photo}/\sigma_{dark}$ |
|---|---|---|
| sputtered a-Si:H | $2\times10^{-8}$ | $7.9\times10^{2}$ |
| glow discharge a-Si:H | $7.4\times10^{-7}$ | $1.3\times10^{3}$ |

## 3. Fabrication and Performance of Schottky and MIS Solar Cells

### 3. 1 Solar Cell Fabrication

Schottky and MIS solar cells were fabricated, using a-Si : H films prepared by rf reactive sputtering and by glow discharge decomposition. For simplicity, a-Si : H films were deposited on $n^+$-Si single-crystal substrates. Vacuum deposited thin gold films with a surface resistivity of 50 ohm/sq. were used as the Schottky barrier metal. Current collection gold electrode patterns with a thickness of 2000Å were also deposited in vacuum.

For the fabrication of Schottky cells, these metal films were directly deposited on the chemically etched surface of the a-Si : H films. The etching was done for 30 sec just before the vacuum deposition, using a solution consisting of HF : $HNO_3$ $CH_3COOH$=3 : 5 : 32.

For MIS cells, the chemically etched surfaces of a-Si : H films were further anodized before deposition of metal films.

In both of Schottky and MIS cells, no anti-reflection coating was provided for easier comparison of cell properties.

### 3. 2 Anodic Oxidation

The anodization set up is schematically shown in Fig.6. The a-Si : H sample to be anodized was fixed on a teflon holder with high-quality wax. The edges of the sample were covered carefully with wax. The electrolyte was a ethylen glycol solution of $KNO_3$ with a concentration of 0.04 mol/*l*. The electrolyte was moderately stirred during anodization. The anode was illuminated by a tungsten lamp at 70000 *lx*. Anodization was tried in both constant-voltage and constant-current modes. In order to limit the value of initial current density in the constant-voltage mode, an external series resistor was inserted in the circuit. Fig.7(a) shows the observed change of anodization current density vs. time in the constant-voltage mode, and Fig. 7 (b) shows that of cell voltage vs. time in the constant-current mode, respec-

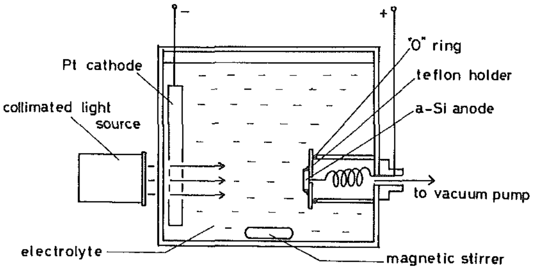

**Fig. 6** Anodization set up

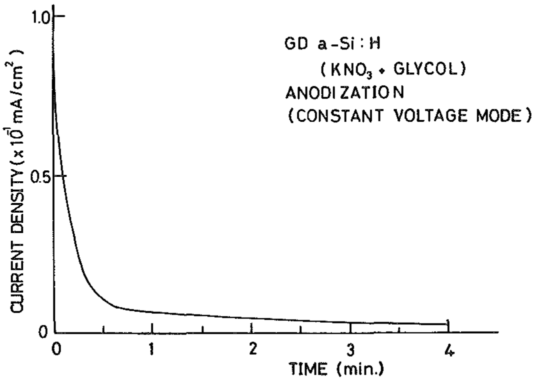

(a) Current vs. time in constant-voltage mode

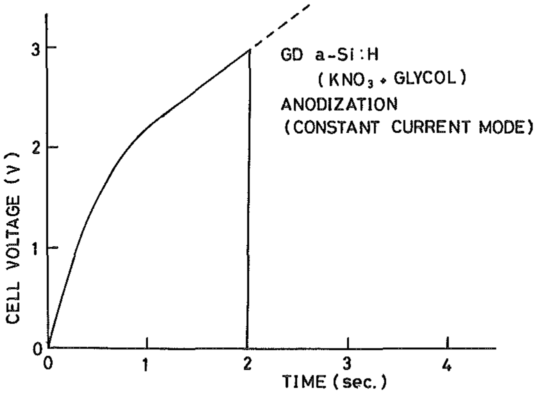

(b) Cell voltage vs. time in constant -current mode

**Fig. 7** Current and voltage behavior during anodization

tively. The anodization behavior shown in Fig. 7(a), (b) is very similar to that of a single-crystal Si recently reported by Nanjo et al.(9).

### 3. 3 Properties of a-Si: H Schottky and MIS Solar Cells

The dark and light I-V characteristics of an a-Si Schottky cell prepared by rf reactive sputtering is shown in Fig.8. The a-Si film thickness is about 3500Å. Fig.9 shows the I-V characteristics under illumination of Schottky and MIS solar cells prepared by glow discharge decomposition. In both cases, illumination was provided by a collimated tungsten lamp. Device notations in Fig.9 and their process conditions are summarized in Table 2. The same device notations are used hereafter.

The detailed dark I-V characteristics of the above rf sputtered and glow discharge decomposed a-Si: H cells are shown in Figs. 10 and 11, respectively. Figure 12

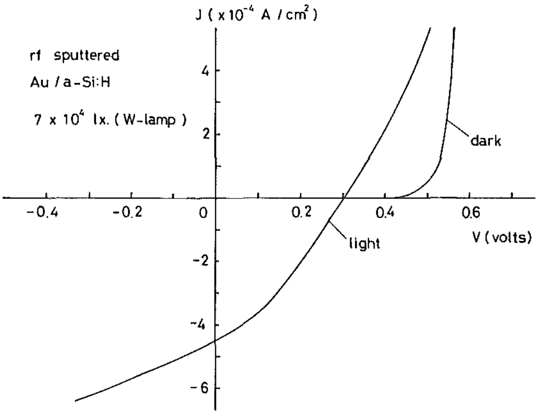

**Fig. 8** Dark and light I-V characteristics of an rf sputtered Au/a-Si: H solar cell

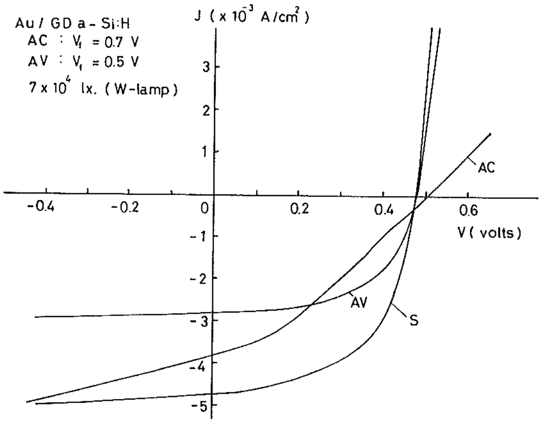

**Fig. 9** Light I-V characteristics of glow discharge Au/a-Si: H Schottky and MIS cells

**Table 2.** Device notations and process conditions of a-Si solar cells

| Notation | Process Conditions |
|---|---|
| S | Schottky ; chemically etched with<br>HF : $HNO_3$ : $CH_3COOH$ = 3 : 5 : 32 (30 sec.) |
| AC | anodization in constant current mode<br>$J_c$ = 0.5 mA/cm$^2$, $V_f$ = 0.7V |
| AV | anodization in constant voltage mode<br>$J_i$ = 0.5 mA/cm$^2$, $V_f$ = 0.5V |

$J_c$ = current density, $J_i$ = initial current density
$V_f$ = fomation voltage

gives the Fowler plots(10) of the zero-bias photocurrent of the same rf sputtered and glow-discharge decomposed cells. From the above experimental results, characteristic quantities of light and dark I-V characteristics are obtained as summarized in Table 3 in terms of the open circuit voltage $V_{oc}$, fill factor F. F., the diode ideality factor n and the barrier heights $\phi_b$ and $\phi_b{}^*$. Here, the barrier height $\phi_b$ and n were determined by applying the standard thermionic emission theory to the linear regions of dark I-V characteristics in Figs.10 and 11 and using the Richardson constant of n-type single-crystal Si of 264 A/cm$^2$K$^2$. On the other hand, $\phi_b{}^*$ denotes the barrier height determined from the internal photoemission data shown in Figs.12 and 13. Since applicability of the ideal thermiotnic emission theory to a-Si Schottky barriers is questionable, $\phi_b{}^*$ appears to be more reliable.

The main observations that can be made from the above experimental results, are as follows:

(1) Although a high photoconductivity was achieved by rf sputtering under

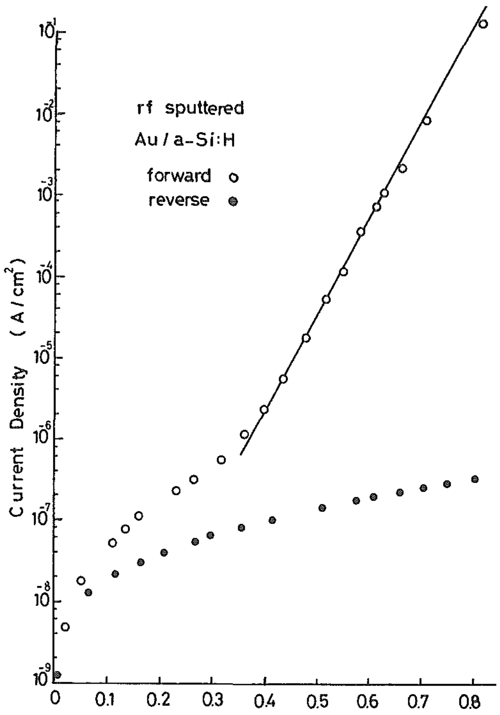

**Fig. 10** Dark I-V characteristics of an rf sputtered Au/Si : H Schottky cell

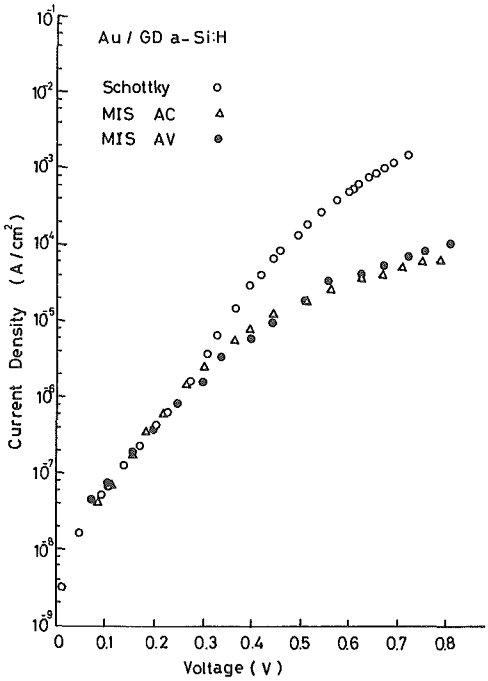

**Fig. 11** Dark I-V characteristics of glow discharge Au/a-Si : H Schottky and MIS cells

**Table 3.** Summary of I-V characteristics of a-Si solar cells

| | | $\phi_b^*$(eV) | $\phi_b$(eV) | n | $V_{oc}$(V) | F.F. |
|---|---|---|---|---|---|---|
| glow discharge a−Si:H | S | 0.91 | 0.95 | 1.66 | 0.48 | 0.56 |
| | AC | 0.96 | 0.92 | 2.26 | 0.50 | 0.37 |
| | AV | 0.88 | 0.91 | 2.45 | 0.48 | 0.49 |
| rf sputtered a−Si:H | S | 1.04 | 1.06 | 1.40 | 0.30 | 0.34 |

optimum conditions, the conversion efficiency of the rf sputtered Schottky solar cell is much smaller than that of the glow discharge decomposed cell. However, it should also be noted that the efficiency of the present rf sputtered cell is much higher than that reported by RCA group(7). This seems to indicate a possibility for further improvement.

(2) Glow discharge decomposition can reproducibly give solar cells of high conversion efficiency (1-2% without AR coating).

(3) Increase of the open-circuit voltage was achieved by anodization in constant current mode. According to Fowler plot analysis in Fig.13, this seems to be due to the increase of barrier height. Reduction of current density is apparently due

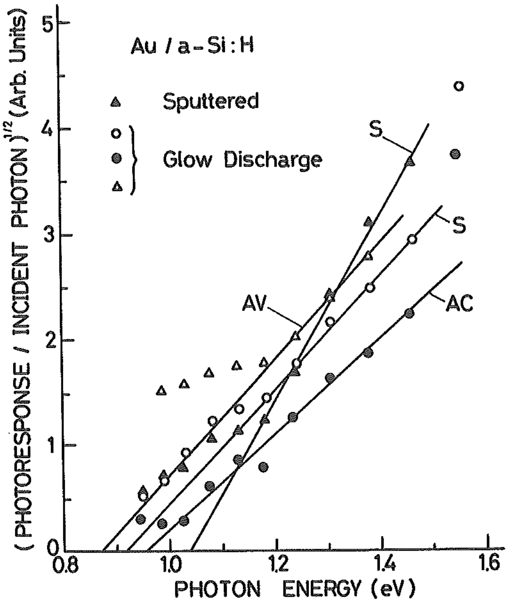

Fig. 12 Fowler plots of zero-bias photocurrent of rf sputtered and glow discharge a-Si : H solar cells.

to deterioration of fill factor which is most probably caused by the series resistance effect, because the thickness of the a-Si film is not optimized as yet. A large deviation of dark I-V characteristics from the linear relationship at higher current densities in Fig.11 indicates the existence of large series resistances.

(4) Dark I-V characteristics of rf sputtered and glow discharge cells are characterized by large values of n in spite of the fact that $\phi_b$ and $\phi_b{}^*$ show reasonably good agreements. This seems to suggest that the current transport in a-Si Schottky and MIS cells are quite different from those of single crystal cells. The rf sputtered cell also showed excess current at a low voltage region as seen in Fig.10. The presence of such a current component was recently reported by Matsunami et al.(11) for single crystal solar cell and interpreted as an indication of surface inversion. Further work seems necessary to fully explain the mechanism of the excess current observed in the present study.

## 4. Conclusion

Hydrogenated amorphous silicon films were prepared by rf sputtering of Si and by glow discharge decomposition of monosilane. It was shown that a-Si : H films of high photoconductivity can be produced under optimized sputtering conditions which are comparable to that of glow discharge decomposition.

Schottky and MIS solar cells were fabricated, using a-Si : H films. Anodization was used for thin insulator film formation using a glycol solution of $KNO_3$. Anodization behavior was found to be similar to that of single crystal silicon. The energy conversion efficiency of glow discharge Schottky cells were found to be approximately ten times larger than that of optimized rf sputtered Schottky cells. Increase of the open-circuit voltage was achieved by anodization in a constant current mode, and this seems to be due to the increase of the barrier height.

Futher work is required for improvements of a-Si film deposition processes and anodization processes, and for the basic understanding of current transport mechanism in a-Si Schottky and MIS diodes.

## Acknowledgement

The present work was financially supported in part by a Grant in-Aid for Special Research on Energy from Ministry of Education, Science and Culture, Japan.

## References

1) D. E. Carlson and C. R. Wronski: Appl. Phys. Lett. **28** (1976) 671.
2) D. L. Pulfley: IEEE Trans. Electron Devices **ED-25** (1978) 1308.
3) H. Hasegawa, S. Tamori and T. Sawada: Jpn. J. Appl. Phys. **19** (1980) Suppl. 19−1, p. 557.
4) H. Yamamoto, M. Moniwa, T. Sawada and H. Hasegawa: Jpn. J. Appl. Phys. **20** (1981) Suppl. 20−2, p. 87.
5) W. E. Spear, P. G. Le Comber, S. Kinmond and M. H. Brodsky: Appl. Phys. Lett. **28** (1976) 105.
6) L. Vieux-Rochaz and A. Chenevas-Paule: J. Non-Cryst. Solids 35 & 36 (1980) 737.
7) D. E. Carlson: IEEE Trans. Electron Devices **ED-24** (1977) 449.
8) T. Imura, K. Mogi and A. Hirai: Proc. 2nd Photovoltaic Sci. and Engin. Conf., Tokyo (1979) 57.
9) J. Nanjo, H. Yamamoto and H, Hasegawa: to be published in Bulletin of the Faculty of Engineering, Hokkaido University, No. 105 (1981).
10) S. M. Sze "Physics of Semiconductor Devices" (John Wiley & Sons, New York, 1969) 404.
11) H. Matsunami, S. Matsumoto and T. Tanaka: Jpn. J. Appl. Phys. **19** (1980) Suppl. 19−2, p. 27.